A Variable Time Gap Feedback Policy for String Stable Adaptive Cruise Control

Shaimaa K. El-Baklish

Anastasios Kouvelas

Michail A. Makridis

STRC conference paper 2024 **April 22, 2024**

STRC | **24th Swiss Transport Research Conference**
Monte Verità / Ascona, May 15-17, 2024

A Variable Time Gap Feedback Policy for String Stable Adaptive Cruise Control

Shaimaa K. El-Baklish
IVT
ETH Zurich
selbaklish@ethz.ch

Anastasios Kouvelas
IVT
ETH Zurich
kouvelas@ethz.ch

Michail A. Makridis
IVT
ETH Zurich
mmakridis@ethz.ch

April 22, 2024

Abstract

In vehicle platooning, time gap settings of Adaptive Cruise Control (ACC) systems have a significant impact on car-following dynamics, traffic capacity and road safety. Traffic capacity increases with the reduction of the average time headway; however, this raises concerns of safety and string stability. This work presents a variable time gap feedback control strategy to balance following a minimum time gap setting under equilibrium car-following conditions for increased traffic capacity; and guaranteeing string stability to attenuate disturbances away from the equilibrium flow. This is achieved using nonlinear $\mathcal{H}_\infty$ control; where a variable time gap component is set as the manipulated control signal. Also, a constant time gap component is present which dominates during car-following equilibrium and is prescribed to the minimum value. Numerical simulations demonstrate that the proposed scheme yields less perturbations in space headway compared to its constant time-gap ACC baseline; showcasing the potential benefits of better road utilization and increased capacity from a traffic perspective.

Keywords

Adaptive Cruise Control (ACC); String Stability; Variable Time Gap; Nonlinear $\mathcal{H}_\infty$ control

Suggested Citation

1 Introduction

Adaptive Cruise Control (ACC) is a part of the advanced driver assistance systems (ADAS) and is designed specifically for vehicle longitudinal control. In fact, ACC systems are the most widespread Society of Engineers (SAE) level 1 automated vehcile (AV) technology in the current markets SAE (2021). For instance, 16 out of 20 best-selling cars in the US market are equipped with an ACC system Shang and Stern (2021). More importantly, vehicle automation gives rise to change traffic flow dynamics and to alleviate instabilities and congestion.

At its center, ACC employs a spacing policy which in turn determines the car-following behavior, platoon stability and traffic efficiency Wu *et al.* (2020). A small inter-vehicular spacing results in a higher traffic capacity but undermines safety and stability. The notion of stability referred to in this work is string stability. Intuitively, vehicles in a platoon are string stable if small perturbations from an equilibrium flow are dampened as they propagate in the upstream direction. Spacing policies in the literature can be categorized into 1) constant spacing (CS), 2) constant time-headway policies (CTH), and 3) variable time-headway (VTH) policies Ntousakis *et al.* (2015). String stability was proved unattainable using CS policy without inter-vehicular communication to provide further information such as leader's acceleration Ntousakis *et al.* (2015); Bian *et al.* (2018). On the other hand, CTH and VTH policies can be appropriately designed to be string stable; nevertheless, there exists the conflicting objective of traffic efficiency. Using the OpenACC database for car-following experiments, the authors in Makridis *et al.* (2021) confirm that a string-stable ACC with large time-headway leads to poor road utilization decreasing capacity. In addition, a large headway threatens drivers' subjective acceptability due to possibly increased lane changes from adjacent lanes Wu *et al.* (2020).

The aim of this work is to develop a VTH policy for ACC which is able to strike a balance between string stability and traffic efficiency. Under equilibrium flow, a CTH policy with a minimum time gap is adopted to promote efficient road utilization by ACC vehicles. This relies on the fact that stable driving conditions are most prevalent. This can also be supported by observed trajectory data from the OpenACC database. Figure 1 shows the distributions of instantaneous acceleration and deceleration which are mostly under ± 0.5 m/s^2 for all platoons in the AstaZero and ZalaZone campaigns. However, perturbations/disturbances give rise to sharp acceleration/deceleration; raising safety, stability and efficiency concerns. Further investigations by Ciuffo et.al. compared short, medium and large time gap settings for field platoons in the ZalaZone experimental campaign in terms of traffic capacity Ciuffo *et al.* (2021). They showed that short time gap platoons are able to attain the highest flow during stable conditions; while highly deteriorating during perturbations to relatively match medium time-gap platoons. Hence, the string instability is detrimental to the potential benefits of ACC systems to traffic flow. Therefore, the CTH policy must to be relaxed to allow for the needed larger gaps to attenuate such disturbances.

Figure 1: Distributions of instantaneous acceleration and deceleration of vehicles per campaign and driving mode. The red labels denote the cumulative proportion of acceleration/deceleration that is below/above ± 0.5 m/s^2.

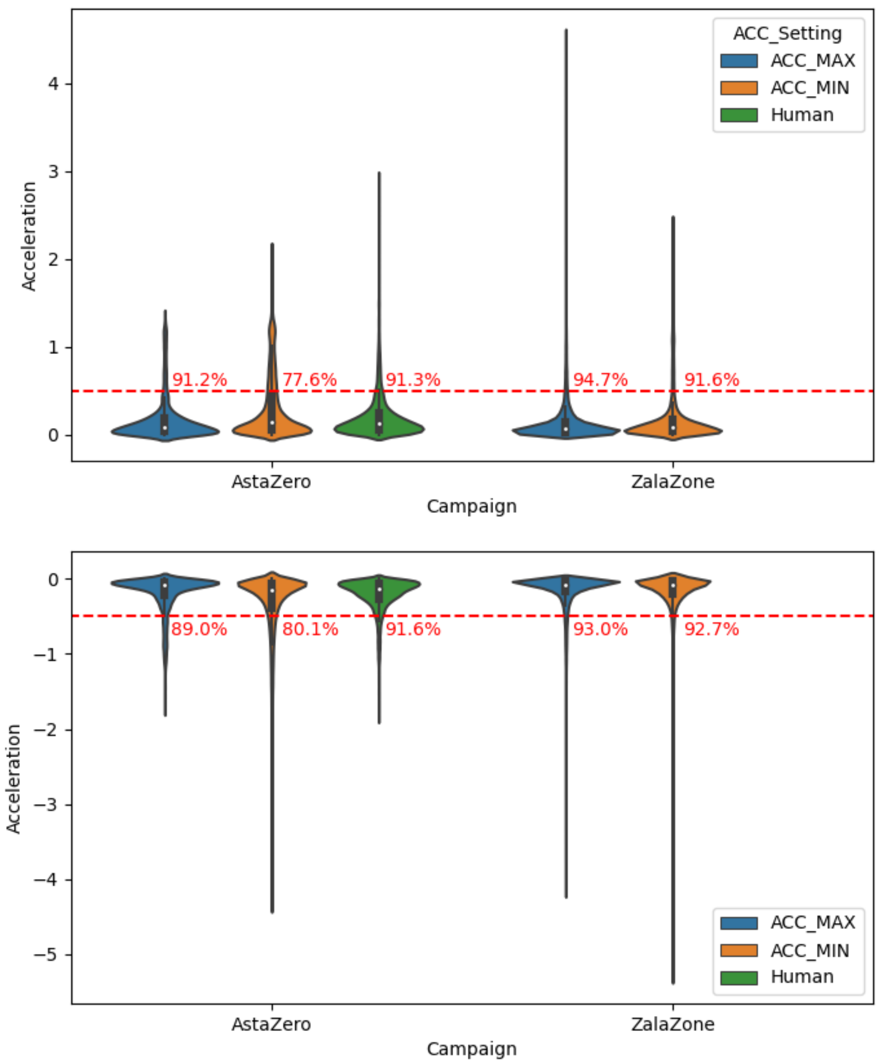

The most widely used ACC model is developed by Milanés and Shladover (2014) as a linear feedback control algorithm; where the acceleration is computed based on deviations away from a target speed (leading vehicle speed in car-following mode) and away from a target spacing determined by a constant time gap (CTG) policy. This spacing policy assumes that the space gap is proportional to the vehicle speed; thus, more appealing to drivers. Furthermore, Gunter et. al. have shown that commercially available ACC systems utilizing CTG policy are string unstable Gunter *et al.* (2021). Interestingly, Shang and Stern (2021) presented simulations of string-unstable ACC vehicles platoon with a minimum time gap which enhanced downstream capacity relative to their string-stable counterpart with a maximum time gap. Lin et.al. demonstrated through experiments the need for different time gap setting in different driving scenarios in order to balance safety and driver's subjective acceptance Lin *et al.* (2009).

Other variable spacing policies assume a nonlinear relationship between the space gap and the vehicle speed to improve stability properties and traffic capacity — e.g. approaches by Wang and Rajamani (2002) and Swaroop and Rajagopal (1999) are inspired by Greenshield's fundamental diagram (FD), approaches by Wang and Rajamani (2002, 2004) and Zhou and Peng (2004) adopt nonlinear spacing policies enforced through sliding mode control and approaches by Kesting *et al.* (2008); Wang *et al.* (2014); Spiliopoulou *et al.* (2018) and Bekiaris-Liberis and Delis (2021) directly manipulate the time gap of the underlying ACC system. Specifically, Bekiaris-Liberis and Delis (2021) assume the time gap of ACC vehicles as a control input to be manipulated to stabilize traffic flow expressed by an Aw-Rascle-Zhang (ARZ) mixed traffic model. The feedback VTG control policy was developed for the linearized system around a uniform, congested equilibrium profile. Numerical simulations reported improved performance in terms of fuel consumption, travel time, and comfort compared to the CTG policy; which the authors proved to yield an unstable traffic flow.

In this work, we employ a VTG policy consisting of both a constant component; which may be a constant desired setting by the driver or a minimum time gap for efficient traffic flow, and a manipulated component to be designed in order to achieve string stability. This manipulated time gap component is developed as a feedback control policy; similar to Bekiaris-Liberis and Delis (2021), using nonlinear $\mathcal{H}_\infty$ control in order to achieve $\mathcal{L}_2$ string stability in the strict sense. A nonlinear analysis is necessary here due to the VTG strategy adopted. Also, formulation through strict string stability facilitates extending the platoon to any number of vehicles; since a platoon can be split to multiple leader-follower subsystems. This scheme provides a compromise between enforcing traffic efficiency during equilibrium car-following conditions and attaining string stability during non-equilibrium flow by relaxation to the VTH policy.

2 Preliminaries

Consider a platoon of $N+1$ vehicles. The leader is denoted by the index 0. Each follower vehicle $i, \forall i = 1, \ldots, N$, is described by the following state-space model.

$$\dot{s}_i(t) = v_{i-1}(t) - v_i(t) \tag{1a}$$

$$\dot{v}_i(t) = f_{a,i}(s_i(t), v_i(t), v_{i-1}(t)) \tag{1b}$$

where s_i and v_i denote the space headway and velocity of vehicle i respectively and v_{i-1} denotes the velocity of the preceding vehicle. The function $f_{a,i}(\cdot)$ represents the longitudinal dynamics defined by car-following models such as the IDM Treiber and Kesting (2013) which may be homogeneous or heterogeneous.

A signal $u(t) \in \mathcal{L}_2$ has, intuitively, bounded energy, i.e. $\int_{t_0}^{\infty} u^T(t)u(t)dt < \infty$, if it belongs to the Lebesgue space $\mathcal{L}_2$ of square-integrable functions.

Definition 1. *Let $s_{eq,i}$ and v_{eq} be the equilibrium profile of (1), $\boldsymbol{x}_i(t) = \begin{bmatrix} s_i(t) - s_{eq,i} & v_i(t) - v_{eq,i} \end{bmatrix}^T$ be the deviation states away from the equilibrium profile and $\delta v_{i-1}(t) = v_{i-1} - v_{eq}$. For any platoon to be strictly input-to-state string-stable, follower vehicle i should have a local $\mathcal{L}_2$-gain equal to or less than $\gamma, \gamma \leq 1$ for any initial state $\boldsymbol{x}_i(0) \in \mathcal{N}$ if the response $\boldsymbol{x}_i(t)$ to any disturbance from the preceding vehicle $\delta v_{i-1}(t) \in \mathcal{L}_2[0, \infty)$ satisfies*

$$\|\boldsymbol{x}_i(t)\|_{\mathcal{L}_2}^2 \leq \gamma^2 \Big(\kappa(\boldsymbol{x}_i(0)) + \|\delta v_{i-1}(t)\|_{\mathcal{L}_2}^2\Big), \forall t \geq 0, i = 1, \ldots, N \tag{2}$$

for some bounded function κ, $\kappa(0) = 0$ and $\mathcal{N} \subseteq \mathcal{X} \subseteq \mathbb{R}^2$ where $\mathcal{X}$ is the set of admissible states.

Definition 2. *Let $\boldsymbol{X}_i(s)$ and $\Delta V_{i-1}(s)$ be the Laplace transform of $\boldsymbol{x}_i(t)$ and $\delta v_{i-1}(t)$. For a linear platoon to be strictly input-to-output string-stable, follower vehicle i should have an $\mathcal{H}_\infty$-norm or induced $\mathcal{L}_2$-gain equal to or less than $\gamma, \gamma \leq 1$ if the response $\boldsymbol{x}_i(t)$ to any disturbance from the preceding vehicle $\delta v_{i-1}(t) \in \mathcal{L}_2[0, \infty)$ satisfies*

$$\|\boldsymbol{\Gamma}_i(s)\|_{\mathcal{H}_\infty} = \sup_{\boldsymbol{\delta v_{i-1}} \in \mathcal{L}_2(0,\infty) \neq 0} \frac{\|\boldsymbol{x}_i(t)\|_{\mathcal{L}_2}^2}{\|\delta v_{i-1}(t)\|_{\mathcal{L}_2}^2} \leq \gamma, \forall i = 1, \ldots, N \tag{3}$$

where $\boldsymbol{\Gamma_i(s)} = \frac{\boldsymbol{X}_i(s)}{\Delta V_{i-1}(s)}$ is the transfer function between follower vehicle i and its predecessor $i-1$.

The $\mathcal{L}_2$-gain, or $\mathcal{H}_\infty$-norm for linear systems, represents the worst-case system gain over all excitations or input disturbances. Thus, if a platoon has an $\mathcal{L}_2$-gain of $\gamma \leq 1$, it means that perturbations will dissipate as they propagate upstream and the platoon will be string-stable.

For a platoon of ACC vehicles Milanés and Shladover (2014), the dynamic model can be written as follows.

$$\dot{s}_i(t) = v_{i-1}(t) - v_i(t) \tag{4a}$$
$$\dot{v}_i(t) = k_{1,i}(s_i(t) - s_0 - L_{i-1} - \tau_i v_i(t)) + k_{2,i}(v_{i-1}(t) - v_i(t)) \tag{4b}$$

where s_0 is the standstill distance, L_{i-1} is the length of vehicle $i-1$ and $k_{1,i}, k_{2,i}$ and τ_i are the spacing control gain, velocity control gain and the constant time gap for ACC vehicle i. The CTG spacing policy is defined as $s_{\text{des},i} = s_0 + L_{i-1} + \tau_i v_i(t)$.

To define the error dynamics of a leader-follower subsystem, the equilibrium profile is defined by the constant speed v_{eq} at which all vehicles are travelling at. The equilibrium space headway is given as $s_{\text{eq},i} = s_0 + L_{i-1} + \tau_i v_{\text{eq}}$. Then, the deviation states are expressed as $\tilde{s}_i = s_i - s_{\text{eq},i}$ and $\tilde{v} = v_i - v_{\text{eq}}$ and the deviation dynamics are derived as follows.

$$\dot{\tilde{s}}_i = v_{i-1} - v_i \tag{5a}$$
$$= (v_{i-1} - v_{\text{eq}}) - (v_i - v_{\text{eq}}) \tag{5b}$$
$$= -\tilde{v}_i + \delta v_{i-1} \tag{5c}$$

$$\dot{\tilde{v}}_i = k_{1,i}(s_i(t) - s_0 - L_{i-1} - \tau_i v_i(t)) + k_{2,i}(v_{i-1}(t) - v_i(t)) \tag{6a}$$
$$= k_{1,i}(s_i(t) - s_0 - L_{i-1} - \tau_i(\tilde{v}_i + v_{\text{eq}})) + k_{2,i}(-\tilde{v}_i + \delta v_{i-1}) \tag{6b}$$
$$= k_{1,i}(s_i(t) - s_0 - L_{i-1} - \tau_i v_{\text{eq}}) - k_{1,i}\tau_i\tilde{v}_i - k_{2,i}\tilde{v}_i + k_{2,i}\delta v_{i-1} \tag{6c}$$
$$= k_{1,i}\tilde{s}_i - k_{1,i}\tau_i\tilde{v}_i - k_{2,i}\tilde{v}_i + k_{2,i}\delta v_{i-1} \tag{6d}$$

where δv_{i-1} denotes the deviation of the leader's velocity away from the equilibrium velocity and represents a disturbance to the considered leader-follower subsystem.

3 Synthesis of $\mathcal{H}_\infty$-based Variable Time Gap Control Policy

In this section, a VTG control policy is designed to guarantee strict string stability during conditions away from the equilibrium profile, $s_{\text{eq},i}$ and v_{eq}, of the ACC model in (4). Consider the following form of the time gap command

$$\tau_i = \tau_i^\star + u_i(t) \tag{7}$$

where $\tau_i^\star$ and $u_i(t)$ are the constant and variable time gap components respectively. The deviation dynamics for follower vehicle i can be then derived similar to (5) and (6) and are expressed as

$$\dot{\tilde{s}}_i(t) = \tilde{v}_i(t) + \delta v_{i-1}(t) \tag{8a}$$

$$\dot{\tilde{v}}_i(t) = k_{1,i}\tilde{s}_i(t) - (k_{1,i}\tau_i^\star + k_{2,i})\tilde{v}_i(t) + k_{2,i}\delta v_{i-1}(t) - k_{1,i}(v_{\text{eq}} + \tilde{v}_i(t))u_i(t) \tag{8b}$$

where $\delta v_{i-1}(t)$ is considered as the disturbance from the preceding vehicle to be attenuated by the control input $u_i(t)$. The system states are denoted by the vector $\boldsymbol{x}_i(t) = \begin{bmatrix} \tilde{s}_i(t) & \tilde{v}_i(t) \end{bmatrix}^T$.

For strict input-to-state string stability, the VTG control policy for $u_i(t)$ needs to be designed to yield an $\mathcal{L}_2$-gain of $\gamma \leq 1$. Notably,the system is nonlinear due to the last term in (8b). To this end, a synthesis of nonlinear $\mathcal{H}_\infty$ controller ensues.

The nonlinear system is represented as in the following standard state-space form

$$\dot{\boldsymbol{x}} = f(\boldsymbol{x}) + g_1(\boldsymbol{x})\boldsymbol{w} + g_2(\boldsymbol{x})\boldsymbol{u} \tag{9a}$$

$$\boldsymbol{z} = h(\boldsymbol{x}) + K_{12}(\boldsymbol{x})\boldsymbol{u} \tag{9b}$$

where the subscript i is dropped for brevity, $\boldsymbol{w} = \delta v_{i-1}$ denotes the exogenous disturbance, $\boldsymbol{u} = u_i$ denotes the control input, and $\boldsymbol{z} = \begin{bmatrix} \rho_s\tilde{s}_i & \rho_v\tilde{v}_i & \rho_u u_i \end{bmatrix}$ denotes the penalty variables with penalty weights of ρ_s, ρ_v and ρ_u. Thus, the vector-valued functions are given as follows.

$$f(\boldsymbol{x}) = \begin{bmatrix} -\tilde{v}_i \\ k_{1,i}\tilde{s}_i - (k_{1,i}\tau_i^\star + k_{2,i})\tilde{v}_i \end{bmatrix} \tag{10a}$$

$$g_1(\boldsymbol{x}) = \begin{bmatrix} 1 \\ k_{2,i} \end{bmatrix} \tag{10b}$$

$$g_2(\boldsymbol{x}) = \begin{bmatrix} 0 \\ -k_{1,i}(v_{\text{eq}} + \tilde{v}_i) \end{bmatrix} \tag{10c}$$

$$h(\boldsymbol{x}) = \begin{bmatrix} \rho_s\tilde{s}_i & \rho_v\tilde{v}_i & 0 \end{bmatrix}^T \tag{10d}$$

$$K_{12}(\boldsymbol{x}) = \begin{bmatrix} 0 & 0 & \rho_u \end{bmatrix}^T \tag{10e}$$

$$h^T(\boldsymbol{x})K_{12}(\boldsymbol{x}) = 0 \ , \ K_{12}^T(\boldsymbol{x})K_{12}(\boldsymbol{x}) = R_2 = \rho_u^2 \tag{10f}$$

The problem of designing $\boldsymbol{u}$ for string stability, as per Definition 1, can be formulated as an infinite-time horizon min-max optimization problem so that the $\mathcal{L}_2$-gain from $\boldsymbol{w}$ to $\boldsymbol{z}$ is $\gamma \leq 1$.

$$\boldsymbol{u}^\star = \arg\min_{\boldsymbol{u}\in\mathcal{U}} \max_{\boldsymbol{w}\in\mathcal{L}_2} \frac{1}{2}\int_0^\infty \|\boldsymbol{z}(t)\|^2 - \gamma^2\|\boldsymbol{w}(t)\|^2 \, dt \text{ subject to (9)} \tag{11}$$

where $\mathcal{U} \subseteq \mathbb{R}$ is the set of admissible control inputs. Here, the objective function balances the minimization of the penalty variables, i.e. performance specifications, against the worst-case exogenous disturbances. Notably, the penalty variables $\boldsymbol{z}(t)$ include the deviation of the space headway away from the equilibrium profile $s_{\text{eq},i}$ and the manipulated time gap command $u_i(t)$. This motivates minimizing the space headway, as an incentive to more efficient road utilization and traffic capacity from a microscopic perspective, and the manipulated time gap command to maintain proximal operating conditions to the constant time gap setting $\tau_i^\star$.

This optimization problem is also a differential game; consisting of a two-player zero-sum game. The minimizing player controls the input $\boldsymbol{u}$; whereas the maximizing player controls the disturbance $\boldsymbol{w}$. This game has a saddle-point equilibrium solution if it has a value function $V : \mathcal{X} \mapsto \mathbb{R}$ that is positive definite and satisfies the Hamilton-Jacobi-Isaacs

(HJI) equation and the optimal feedback policies of both players Huang and Lin (1995)

$$\boldsymbol{u}^\star = -R_2^{-1}(\boldsymbol{x})g_2^T(\boldsymbol{x})V_x \tag{12a}$$
$$\boldsymbol{w}^\star = \frac{1}{\gamma^2}g_1^T(\boldsymbol{x})V_x \tag{12b}$$
$$V_x f(\boldsymbol{x}) + \frac{1}{2}h^T(\boldsymbol{x})h(\boldsymbol{x}) + \frac{1}{2}V_x\Big(\frac{1}{\gamma^2}g_1(\boldsymbol{x})g_1^T(\boldsymbol{x}) - g_2(\boldsymbol{x})R_2^{-1}g_2^T(\boldsymbol{x})\Big) = 0 \tag{12c}$$

where V_x is the Jacobian matrix of $V(\boldsymbol{x})$. A closed form solution for (12c) does not exist, thus, a numerical approximation using Taylor's series is adopted. Then, the HJI equation becomes an algebraic Ricatti equation of the following form to be solved online; since we consider the equilibrium velocity as the subsystem leader velocity $v_{\text{eq}} = v_{i-1}$.

$$PA + A^TP + P\left(\frac{1}{\gamma^2}B_1B_1^T - B_2R_2^{-1}B_2^T\right)P + C^TC = 0 \tag{13a}$$
$$f(\boldsymbol{x}_i) = A\boldsymbol{x}_i + \hat{f}^{[2+]}(\boldsymbol{x}_i)\ ;\ A = \begin{bmatrix} 0 & -1 \\ k_1 & -(k_1T_g^\star + k_2) \end{bmatrix} \tag{13b}$$
$$g_1(\boldsymbol{x}_i) = B_1 + \hat{g}_1^{[1+]}(\boldsymbol{x}_i)\ ;\ B_1 = \begin{bmatrix} 1 \\ k_2 \end{bmatrix} \tag{13c}$$
$$g_2(\boldsymbol{x}_i) = B_2 + \hat{g}_2^{[1+]}(\boldsymbol{x}_i)\ ;\ B_2 = \begin{bmatrix} 0 \\ -k_1v_e \end{bmatrix} \tag{13d}$$
$$h(\boldsymbol{x}_i) = C\boldsymbol{x}_i + \hat{h}^{[2+]}(\boldsymbol{x}_i)\ ;\ C = \begin{bmatrix} \rho_s & 0 \\ 0 & \rho_v \\ 0 & 0 \end{bmatrix} \tag{13e}$$
$$V(\boldsymbol{x}_i) = \boldsymbol{x}_i^TP\boldsymbol{x}_i + \hat{V}^{[3+]}(\boldsymbol{x}_i) \tag{13f}$$

The n^{th}-order and higher-order terms of the function $(\cdot)(\boldsymbol{x}_i)$ are denoted by $\hat{(\cdot)}^{[n+]}(\boldsymbol{x}_i)$ and $P \succeq 0$ is a symmteric positive definite matrix. Note that, in our setting, the only assumptions made are (13d) and (13f) and the rest are exact expressions. On another note, the algebraic Ricatti equation in (13a) is feasible for a prescribed γ if the pair (A, B_2) is stabilizable and the Hamiltonian matrix

$$H = \begin{bmatrix} A & \left(\frac{1}{\gamma^2}B_1B_1^T - B_2R_2^{-1}B_2^T\right) \\ -C^TC & -A^T \end{bmatrix}$$

is dichotomic, i.e. has no eigenvalues on the imaginary axis. This is true for $v_{\text{eq}} > 0$ and for an appropiate choice of penalty weights, ρ_s, ρ_v and ρ_u. The VTG control strategy can be illustrated in Figure 2.

Figure 2: Block diagram of the VTG proposed feedback control policy.

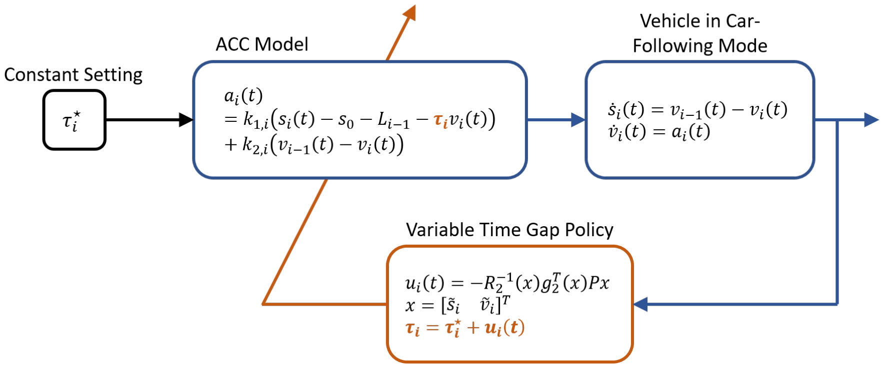

This VTG policy is robust to velocity disturbances from the leader away from the equilibrium profile; thus it yields a string-stable system in the strict sense with a worst case $\mathcal{L}_2$-gain of $\gamma \leq 1$. It also guarantees the internal stability of the considered vehicle i. Additionally, the constant time gap setting can be kept either at minimum setting for benefits in traffic efficiency or at a desired setting chosen by the driver. Hence, the time gap parameter design is modularized by separating string stability from other considerations.

4 Numerical Simulations

In this section, the performance of the proposed VTG ACC scheme will be investigated against the CTG ACC scheme Milanés and Shladover (2014) and two string-stable controllers from the literature Zhou and Peng (2004); Mousavi *et al.* (2023) on artificial driving cycles.

The first ACC scheme by Zhou and Peng (2004) utilizes a quadratic spacing policy inspired from human driving behavior and optimized for string stability and maximum traffic capacity. The desired space headway $s_{\text{des},i}(t)$ according to the spacing policy can be expressed as

$$s_{\text{des},i}(t) = L_{i-1} + A + Tv_i(t) + Gv_i^2(t) \tag{14}$$

where A is the standstill distance and $T = 0.0019$ and $G = 0.0448$ are coefficients identified by the authors through constrained optimization. A sliding mode controller is implemented to find the follower acceleration enforcing such spacing policy. The car-following dynamics in (1) beocmes

$$f_{a,i}(s_i(t), v_i(t), v_{i-1}(t)) = \frac{\lambda}{T + 2Gv_i(t)}(s_i(t) - s_{\text{des},i}(t)) + \frac{1}{T + 2Gv_i(t)}(v_{i-1}(t) - v_i(t)) \quad (15)$$

where λ is a controller gain defining the sliding surface dynamics $\dot{\epsilon} = -\lambda\epsilon$. The sliding variable ϵ is expressed through deviation of space headway away from desired spacing $\epsilon = s_i(t) - s_{\text{des},i}(t)$. This essentially implements a VTG policy and will be referred to as VTG SMC. Also, Table 1 summarizes the used parameter values for all ACC schemes investigated.

Table 1: Parameter values of the implemented ACC control schemes.

CTG ACC		VTG ACC		VTG SMC		Centralized ACC	
Parameter	Value	Parameter	Value	Parameter	Value	Parameter	Value
k_1	0.23	k_1	0.23	λ	2	ρ_s	0.2
k_2	0.07	k_2	0.07	T	0.0019	ρ_v	0.3
τ	1.0	$\tau^\star$	1.0	G	0.0448	ρ_u	1
s_0	3	s_0	3	A	3		
L	5	ρ_s	0.2	L	5		
		ρ_v	0.3				
		ρ_u	1				
		γ	0.95				

Figure 3 shows the resulting trajectories of 4 following vehicles of a platoon leader, with the lead velocity shown in black, on a straight open road. The following vehicles start with an initial perturbation in their velocities. This driving cycle, also, has sharp acceleration/deceleration of maximum values ± 4 m/s^2 at $t = 50, 300$ s; thus, the response to different types of disturbances can be observed. The minimum time-gap setting of $\tau = \tau^\star = 1$ s was used. Naturally, the CTG ACC shows string-unstable behavior; where the perturbations in both velocity and spacing amplify as they propagate upstream. On the other hand, both VTG ACC and VTG SMC are string-stable. Nevertheless, VTG SMC demonstrates larger space gaps to accommodate and dissipate these disturbances; whereas, the proposed VTG ACC scheme introduces minimal changes in space and time headways with respect to the equilibrium minimum time gap operation. It is, also, important to notice that the amplified oscillations exhibited by CTG ACC present with dangerously low values of time headway raising safety concerns. This highlights the importance of the choice of the penalty variables $\boldsymbol{z}(t)$ in the optimization problem (11) and the design of the nonlinear $\mathcal{H}_\infty$ scheme.

Figure 3: Simulated trajectories of a platoon of 5 vehicles along a straight road using CTG ACC, VTG SMC and the proposed VTG ACC. Platoon leader velocity is the black dashed line.

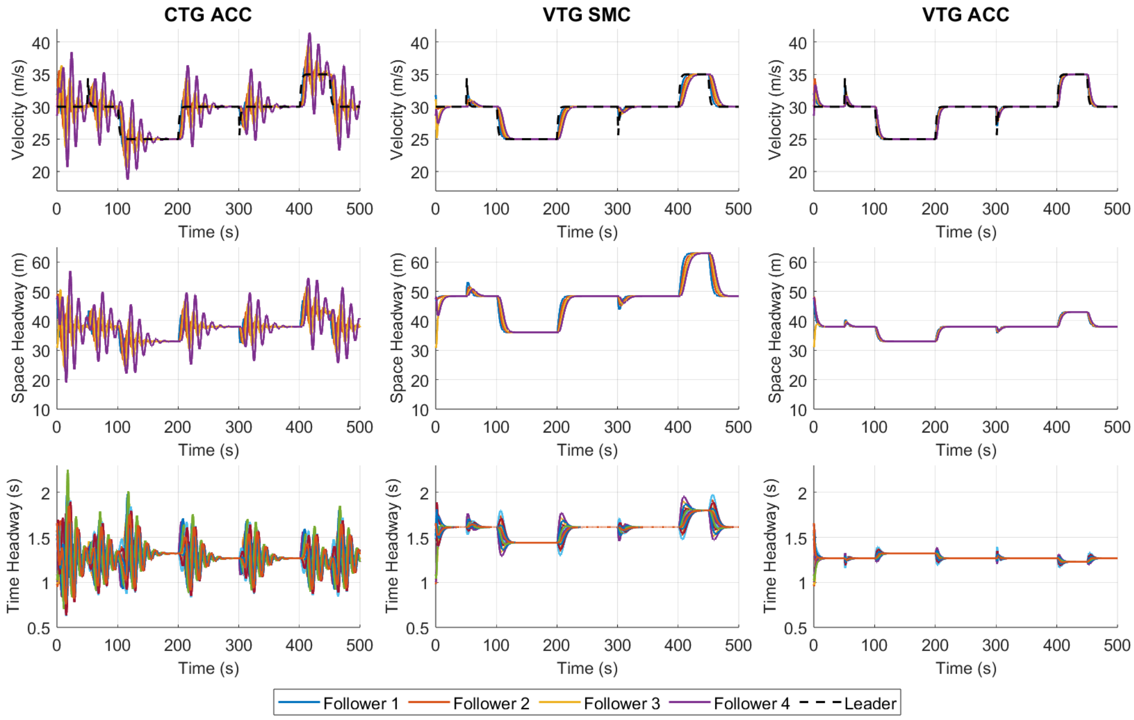

Additionally, in order to asses the safety and energy consumption of these approaches, the Time To Collision TTC_i and tractive energy consumption E_i metrics were used. The instantaneous TTC can be expressed as

$$TTC_i(t) = \frac{s_i(t) - L_{i-1}}{v_i(t) - v_{i-1}(t)} \tag{16}$$

whereas the tractive energy consumption is obtained as follows Apostolakis and Ampountolas (2023).

$$P_i = \max\Big(0, 10^{-3} v_i \big(F_0 + F_1 v_i + F_2 V_i^2 + 1.03 m a_i + m g \sin\theta\big)\Big) \tag{17a}$$

$$E_i = \frac{\int_0^T P_i dt}{0.036 \int_0^T v_i dt} \tag{17b}$$

Tractive energy consumption takes into account only tractive power demand so that it is agnostic to vehicle specifications; enabling a fair comparison between different ACC algorithms. The road is assumed horizontal; $\theta = 0$. The road-related coefficients $F_0 = 213$ N, $F_1 = 0.0861$ Ns/m, $F_2 = 0.0027\text{Ns}^2/\text{m}^2$ and the vehicle's mass $m = 1500$ kg are assumed constant over all vehicles in order to normalize over the different platoons and compare the performance of the utilized ACC algorithms. Figure 4 illustrates the minimum TTC and tractive energy consumption of each vehicle inside the platoons. For the first following vehicle, the proposed scheme yields an improved TTC by 86.4% compared to CTG ACC and by 23.5% compared to VTG SMC. This difference is quite pronounced for the first follower since it is the immediate following vehicle to the perturbing one (i.e. platoon leader). Regarding tractive energy consumption, both the VTG ACC and VTG SMC algorithms homogenize the energy consumption overall the platoon members; whereas the CTG ACC algorithm shows higher energy consumption due to the disturbances propagation along the platoon. Hence, safety and energy efficiency concerns raised due to string instability are releived using the proposed approach while optimizing road space utilization by adhering to a minimum time gap during stable car-following conditions.

Figure 4: Time To Collision and tractive energy consumption of followers in a platoon of 5 vehicles along a straight road using CTG ACC, VTG SMC and the proposed VTG ACC.

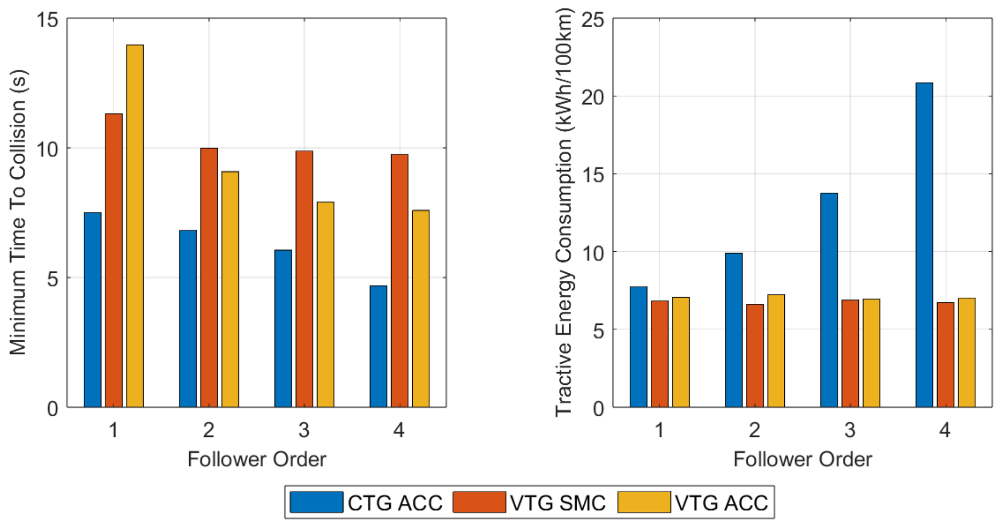

As for the approach adopted by Mousavi et.al. Mousavi *et al.* (2023), a centralized mixed $\mathcal{H}_2/\mathcal{H}_\infty$ control strategy is developed for a platoon of heterogeneous vehicles to mitigate the effect of disturbances and regulate the platoon to equilibrium flow. Here, we consider homogeneous platoons of ACC-enabled vehicles for implementation of the centralized controller by Mousavi *et al.* (2023) for comparison. This test is carried out for a platoon of 5 vehicles in a ring road of length 165 m as well as a minimum time gap of $\tau = \tau^\star = 1$ s. Initial perturbations in the vehicles velocities are introduced as well as a sharp deceleration of -3 m/s^2 lasting 3 s for one random vehicle — 'CAV3' in Figure 5.

As illustrated in Figure 5, both schemes are able to dissipate perturbations as they are string stable by design. However, the centralized ACC algorithm shows lower changes in space and time headway relative to the proposed VTG ACC algorithm. The reason is that the former scheme assumes a centralized cooperative structure; therefore, has global information about all platoon vehicles. In contrast, our proposed control scheme is completely decentralized via predecessor-follower topology and only needs sensor measurements of spacing and lead velocity; thus, it is more computationally efficient with comparable performance.

Figure 5: Simulated trajectories of the (a) first and (b) last followers in a platoon of 5 vehicles along a straight road using CTG ACC, VTG SMC and the proposed VTG ACC. Platoon leader velocity is the black dashed line.

(a) Centralized $\mathcal{H}_2/\mathcal{H}_\infty$ ACC scheme

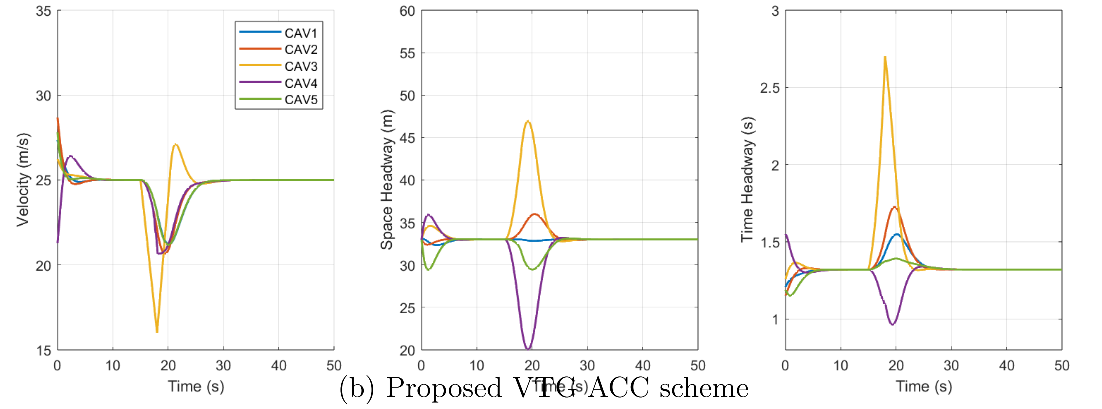

(b) Proposed VTG ACC scheme

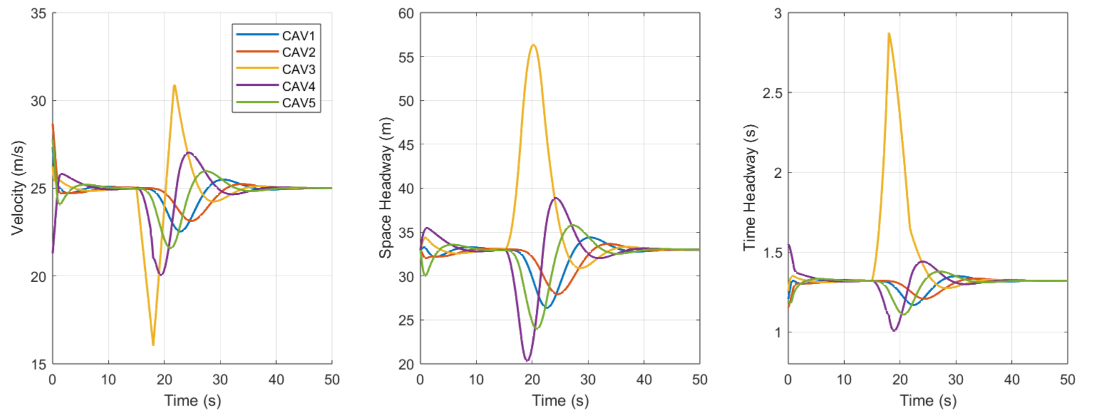

5 Conclusion

In this article, a variable time gap strategy is designed to guarantee string stability in the strict sense for vehicle platoons. The control architecture is modular; where a constant time gap component $\tau^\star$ and a variable time gap component $u(t)$ is designed as the control policy for disturbance attenuation. Strict string stability is guaranteed through nonlinear $\mathcal{H}_\infty$ control to dissipate perturbations from the leading vehicle to the prescribed penalty variables; space headway and ego vehicle's velocity. The string stability problem is decoupled from equilibrium flow dictated by $\tau^\star$; which may define driver comfort settings or a minimum time gap value for traffic efficiency. The performance of the proposed scheme is validated through numerical simulations. Due its projected benefits, the proposed ACC algorithm is yet to be validated versus commercially available ACC systems through both numerical and microscopic traffic simulations in multiple scenario to compare these benefits in terms of traffic efficiency, safety and energy consumption.

6 References

Apostolakis, T. and K. Ampountolas (2023) Physics-inspired neural networks for parameter learning of adaptive cruise control systems, 9 2023.

Bekiaris-Liberis, N. and A. I. Delis (2021) Pde-based feedback control of freeway traffic flow via time-gap manipulation of acc-equipped vehicles, *IEEE Transactions on Control Systems Technology*, **29**, 461–469, ISSN 15580865.

Bian, Y., Y. Zheng, S. E. Li, Z. Wang, Q. Xu, J. Wang and K. Li (2018) Reducing time headway for platoons of connected vehicles via multiple-predecessor following, *IEEE Conference on Intelligent Transportation Systems, Proceedings, ITSC*, **2018-November**, 1240–1245, 12 2018.

Ciuffo, B., K. Mattas, M. Makridis, G. Albano, A. Anesiadou, Y. He, S. Josvai, D. Komnos, M. Pataki, S. Vass and Z. Szalay (2021) Requiem on the positive effects of commercial adaptive cruise control on motorway traffic and recommendations for future automated driving systems, *Transportation Research Part C: Emerging Technologies*, **130**, 103305, 9 2021, ISSN 0968-090X.

Gunter, G., D. Gloudemans, R. E. Stern, S. McQuade, R. Bhadani, M. Bunting, M. L. D. Monache, R. Lysecky, B. Seibold, J. Sprinkle, B. Piccoli and D. B. Work (2021) Are commercially implemented adaptive cruise control systems string stable?, *IEEE Transactions on Intelligent Transportation Systems*, **22**, 6992–7003, ISSN 15580016.

Huang, J. and C. F. Lin (1995) Numerical approach to computing nonlinear $\mathcal{H}_\infty$ control laws, *Journal of Guidance, Control, and Dynamics*, **18**, 989–994, ISSN 07315090.

Kesting, A., M. Treiber, M. Schönhof and D. Helbing (2008) Adaptive cruise control design for active congestion avoidance, *Transportation Research Part C: Emerging Technologies*, **16**, 668–683, ISSN 0968090X.

Lin, T. W., S. L. Hwang and P. A. Green (2009) Effects of time-gap settings of adaptive cruise control (acc) on driving performance and subjective acceptance in a bus driving simulator, *Safety Science*, **47**, 620–625, 5 2009, ISSN 0925-7535.

Makridis, M., K. Mattas, A. Anesiadou and B. Ciuffo (2021) Openacc. an open database of car-following experiments to study the properties of commercial acc systems, *Transportation Research Part C: Emerging Technologies*, **125**, 103047, ISSN 0968090X.

Milanés, V. and S. E. Shladover (2014) Modeling cooperative and autonomous adaptive cruise control dynamic responses using experimental data, *Transportation Research Part C: Emerging Technologies*, **48**, 285–300, ISSN 0968090X.

Mousavi, S. S., S. Bahrami and A. Kouvelas (2023) A mixed $\mathcal{H}_2/\mathcal{H}_\infty$ controller design for a platoon with multiple human-driven and connected and automated vehicles, *2023 European Control Conference, ECC 2023*.

Ntousakis, I. A., I. K. Nikolos and M. Papageorgiou (2015) On microscopic modelling of adaptive cruise control systems, *Transportation Research Procedia*, **6**, 111–127, ISSN 23521465.

SAE (2021) Society of Automotive Engineers J3016: Taxonomy and definitions for terms related to driving automation systems for on-road motor vehicles, `https://www.sae.org/standards/content/j3016_202104/`.

Shang, M. and R. E. Stern (2021) Impacts of commercially available adaptive cruise control vehicles on highway stability and throughput, *Transportation Research Part C: Emerging Technologies*, **122**, 102897, 1 2021, ISSN 0968-090X.

Spiliopoulou, A., D. Manolis, F. Vandorou and M. Papageorgiou (2018) Adaptive cruise control operation for improved motorway traffic flow, *Transportation Research Record*, **2672**, 24–35, ISSN 21694052.

Swaroop, D. and K. R. Rajagopal (1999) Intelligent cruise control systems and traffic flow behavior, *ASME International Mechanical Engineering Congress and Exposition, Proceedings (IMECE)*, **1999-J**, 373–380.

Treiber, M. and A. Kesting (2013) *Traffic Flow Dynamics*, ISBN 9783642324598.

Wang, J. and R. Rajamani (2002) Adaptive cruise control system design and its impact on highway traffic flow, *Proceedings of the American Control Conference*, **5**, 3690–3695, ISSN 07431619.

Wang, J. and R. Rajamani (2004) Should adaptive cruise-control systems be designed to maintain a constant time gap between vehicles?, *IEEE Transactions on Vehicular Technology*, **53**, 1480–1490, ISSN 00189545.

Wang, M., W. Daamen, S. P. Hoogendoorn and B. van Arem (2014) Rolling horizon control framework for driver assistance systems. part i: Mathematical formulation and non-cooperative systems, *Transportation Research Part C: Emerging Technologies*, **40**, 271–289, ISSN 0968090X.

Wu, C., Z. Xu, Y. Liu, C. Fu, K. Li and M. Hu (2020) Spacing policies for adaptive cruise control: A survey, *IEEE Access*, **8**, 50149–50162, ISSN 21693536.

Zhou, J. and H. Peng (2004) Range policy of adaptive cruise control for improved flow stability and string stability, *Conference Proceeding - IEEE International Conference on Networking, Sensing and Control*, **1**, 595–600.